Exact solutions and topological phase diagram in interacting dimerized Kitaev topological superconductors

Motohiko Ezawa

Phys. Rev. B **96**, 121105 — Published 8 September 2017

DOI: 10.1103/PhysRevB.96.121105

Exact solutions and topological phase diagram in interacting dimerized Kitaev topological superconductors

Motohiko Ezawa

It was recently shown that an interacting Kitaev topological superconductor model is exactly solvable based on two-step Jordan-Wigner transformations together with one spin rotation. We generalize this model by including the dimerization, which is shown also to be exactly solvable. We analytically determine the topological phase diagram containing seven distinct phases. It is argued that the system is topological when a fermionic many-body Majorana zero-energy edge state emerges. It is intriguing that there are two tetra-critical points, at each of which four distinct phases touch.

Introduction: Majorana fermions were used for the first time in condensed matter physics to exactly solve the two-dimensional Ising model by mapping it to the one-dimensional quantum spin model[1] with the use of the Jordan-Wigner transformation[2,3]. Recently, a renewed interest on Majorana fermions has created one of the most active fields in the context of topological superconductors[4–6]. They are expected to play a key role in future topological quantum computations[7]. The Kitaev topological superconductor (KTSC) model is a fundamental one which hosts Majorana fermions[8]. It is exactly solvable since it describes free electrons. An interplay between topology and interaction is a fascinating subject. There are several works where electron-electron interaction effects have been investigated[9–22]. It is shown[13,15,16] that there is a topological phase transition between a topological superconductor (TSC) state and trivial charge-density wave (CDW) state at a certain interaction strength.

The KTSC model is characterized by the three parameters, i.e., the transfer integral t, the superconducting pairing gap Δ and the chemical potential μ. The system is topological for $|\mu| < 2t$, while it is trivial for $|\mu| > 2t$. The interacting KTSC model contains an additional electron-electron interaction U. It is exactly solvable under the frustration free condition[23], i.e., $\mu = 4\sqrt{U^2 + tU + (t^2 - \Delta^2)/4}$. It is also exactly solvable at the symmetric point[10] $\Delta = U = t$ and $\mu = 0$. Recently, this exact solution is extended for $\Delta = t$ and $\mu = 0$ with an arbitrary U by mapping the system to the KTSC model[24] with the aid of the combination of two-step Jordan-Wigner transformations and one spin rotation. This method is also applicable to the KTSC model with disorders[25].

In this paper, we generalize the interacting KTSC model by including the dimerization with parameter η, $|\eta| \leq 1$. The model is exactly solvable for the case of $\Delta = t$ and $\mu = 0$ with an arbitrary U. We analytically obtain the topological phase diagram in the (U/t)-η plane, which contains seven distinct phases. The topological properties of each phase are determined based on the bulk-edge correspondence. It is argued that the emergence of a fermionic many-body Majorana zero-energy edge state is a manifestation of the topological nontriviality of the system. We also discuss the duality relation between topological phases.

Hamiltonian: We consider a one-dimensional chain of spinless electrons: See Fig.1. The tight-binding model for a hybrid system comprised of the Kitaev model[8] and the Su-Schrieffer-Heager (SSH) model[26] together with the electron-electron interaction is given by

$$\begin{aligned} H =& -\mu \sum_j c_j^\dagger c_j - \sum_j t_j (c_j^\dagger c_{j+1} + \text{h.c.}) \\ & - \sum_j \Delta_j (c_j^\dagger c_{j+1}^\dagger + \text{h.c.}) \\ & + \sum_j U_j \left(2c_j^\dagger c_j - 1\right)\left(2c_{j+1}^\dagger c_{j+1} - 1\right), \end{aligned} \tag{1}$$

with

$$\begin{aligned} t_j &= t\left\{1 - \eta\,(-1)^j\right\}, \qquad \Delta_j = \Delta\left\{1 - \eta\,(-1)^j\right\}, \\ U_j &= U\left\{1 - \eta\,(-1)^j\right\}, \end{aligned} \tag{2}$$

where μ is the chemical potential, t is the transfer integral, and Δ is the superconducting pairing gap taken to be real. Parameters t_j, Δ_j and U_j are dependent of sites due to the dimerization η. We assume $t \geq 0$ without loss of generality, since the local unitary transformation $c_j \to -i\,(-1)^j\, c_j$ interchanges t and $-t$. In addition, we assume $\Delta \geq 0$ since the phase transformation $c_j \to i c_j$ interchanges Δ and $-\Delta$. Without the interaction this Hamiltonian is reduced to the dimerized KTSC model[27].

Jordan-Wigner transformation: The model with no dimerization is exactly solvable[24] for the case of $\Delta = t$ and $\mu = 0$. We now show that, even if we include the dimerization η, it is exactly solvable for the case of $\Delta = t$ and $\mu = 0$. We consider the Jordan-Wigner transformation[13,15,19,23,24,28], representing the fermion operators in terms of the spin operator, such that $c_i = K_i \sigma_i^-$ and $c_i^\dagger = \sigma_i^+ K_i^\dagger$, with $K_i = \prod_{j=-M}^{i-1} \left(-\sigma_j^z\right)$ and $\sigma_i^\pm = \sigma_i^x \pm i\sigma_i^y$. It follows that

$$\sigma_j^x \sigma_{j+1}^x = c_j^\dagger c_{j+1} + c_{j+1}^\dagger c_j + c_j^\dagger c_{j+1}^\dagger + c_{j+1} c_j, \tag{3}$$

and

$$\sigma_j^z \sigma_{j+1}^z = \left(2c_j^\dagger c_j - 1\right)\left(2c_{j+1}^\dagger c_{j+1} - 1\right). \tag{4}$$

The Hamiltonian is rewritten in terms of the spin operator as

$$H = \sum_j (-t_j \sigma_j^x \sigma_{j+1}^x + U_j \sigma_j^z \sigma_{j+1}^z), \tag{5}$$

which is the XZ spin model with dimerization[29]. It is customary to make a spin rotation[24,30] by $\pi/2$ around the x axis

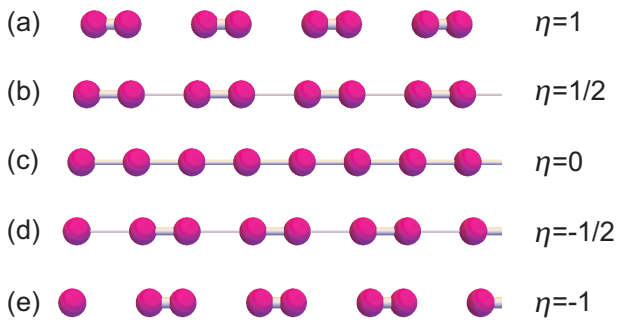

FIG. 1: Illustration of a semi-infinite chain of spinless electrons for various dimerization η. For the case $\eta=-1$, the edge site is isolated, leading to the SSH-like zero-energy edge state.

using the rotation operator $R=\exp\left[-i\pi/2\sum_j \sigma_j^x\right]$, and obtain the XY model with dimerization,

$$H=\sum_j(-t_j\sigma_j^x\sigma_{j+1}^x+U_j\sigma_j^y\sigma_{j+1}^y). \tag{6}$$

We further make the inverse Jordan-Wigner transformation,

$$\sigma_i^x = \frac{1}{2}\left(f_i^\dagger+f_i\right)\exp\left[i\pi\sum_i^{j-1}f_j^\dagger f_j\right], \tag{7}$$

$$\sigma_i^y = \frac{1}{2i}\left(f_i^\dagger-f_i\right)\exp\left[i\pi\sum_i^{j-1}f_j^\dagger f_j\right], \tag{8}$$

$$\sigma_i^z = f_i^\dagger f_i-\frac{1}{2}. \tag{9}$$

The Hamiltonian turns out to be

$$H=\sum_j[-\left(t_j-U_j\right)f_j^\dagger f_{j+1}-\left(t_j+U_j\right)f_j^\dagger f_{j+1}^\dagger+\text{h.c.}]. \tag{10}$$

This is solved explicitly as follows.

Phase diagram: The system has two sublattices A and B made of the odd and even number sites in the presence of the dimerization. Indeed, the parameters t_j, Δ_j and U_j in the Hamiltonian (1) are common in each sublattice, i.e., $t_j=t_{A(B)}$, $\Delta_j=\Delta_{A(B)}$ and $U_j=U_{A(B)}$ for all j belonging to the sublattice $A(B)$. Introducing the four-component operator $C_k^\dagger=(f_{kA}^\dagger,f_{kB}^\dagger,f_{-kA},f_{-kB})$, where A and B denote the odd and even number sites, we express the Hamiltonian H in the Bogoliubov-de Gennes form. We obtain

$$H=\frac{1}{2}\sum_k C_k^\dagger\mathcal{H}\left(k\right)C_k \tag{11}$$

in the momentum space, with

$$\mathcal{H}\left(k\right)=\begin{pmatrix}0 & z & 0 & w\\ z^* & 0 & -w^* & 0\\ 0 & -w & 0 & -z\\ w^* & 0 & -z^* & 0\end{pmatrix}, \tag{12}$$

where

$$z\left(k\right)=-(t+U)\left[(1+\eta)+(1-\eta)\,e^{-ika}\right], \tag{13}$$

$$w\left(k\right)=-(t-U)\left[(1+\eta)-(1-\eta)\,e^{-ika}\right], \tag{14}$$

and a is the lattice constant. Diagonalizing this Hamiltonian we obtain the eigenvalues and the eigenfunctions explicitly.

In particular, the eigenvalues are

$$E^2\left(k\right)/4=\left(1\pm\eta\right)^2t^2+\left(1\mp\eta\right)^2U^2-2tU\left(1-\eta^2\right)\cos k. \tag{15}$$

The gap closes for

$$\eta=\pm\left(t-U\right)/\left(t+U\right),\quad \pm\left(t+U\right)/\left(t-U\right). \tag{16}$$

These gap-closing conditions generate the phase boundaries. There are seven distinct phases as in Fig.2(a).

Our next task is to determine the topological properties of each phase. However, we cannot discuss the topological properties of the original system with the use of the Jordan-Wigner transformed operator f_j since it is given by a non-local transformation. Note that the topological properties are not conserved by such a transformation[31]. Nevertheless, it is possible to discuss them by examining the edge state[25] based on the bulk-edge correspondence by considering a semi-infinite chain with one edge.

Majorana edge states: First we show that there are two types of edge states. We introduce the Majorana representation $\lambda_j^A=f_j^\dagger+f_j$ and $\lambda_j^B=i(f_j^\dagger-f_j)$, and rewrite the Hamiltonian (10) in the Majorana form,

$$H=i\sum_j t_j\lambda_j^B\lambda_{j+1}^A+U_j\lambda_j^A\lambda_{j+1}^B. \tag{17}$$

This is separated into two independent Hamiltonias[25] as $H=H_I+H_{II}$ with

$$H_I=\sum_j it_{2j}\phi_{I,j}^B\phi_{I,j+1}^A+iU_{2j-1}\phi_{I,j}^A\phi_{I,j}^B, \tag{18}$$

$$H_{II}=\sum_j -iU_{2j}\phi_{II,j}^B\phi_{II,j+1}^A-it_{2j-1}\phi_{II,j}^A\phi_{II,j}^B, \tag{19}$$

where we have defined $\phi_{I,j}^A=\lambda_{2j-1}^A$, $\phi_{I,j}^B=\lambda_{2j}^B$, $\phi_{II,j}^A=\lambda_{2j-1}^B$ and $\phi_{II,j}^B=\lambda_{2j}^A$. This decoupling is in essence of the relation between the XY model in zero field and two independent transverse-field Ising models[32,33].

The Jordan-Wigner transformed Majorana operators λ_ν^μ are written in terms of the original Majorana operators as[24,25]

$$\phi_{I,j}^A=\lambda_{2j-1}^A=\gamma_1^B\prod_{k=1}^{j-3}[i\gamma_{2k}^A\gamma_{2k+1}^B](i\gamma_{j-1}^A\gamma_j^A), \tag{20}$$

$$\phi_{I,j}^B=\lambda_{2j}^B=\gamma_1^B\prod_{k=1}^{j-2}[i\gamma_{2k}^A\gamma_{2k+1}^B](i\gamma_j^A\gamma_j^B), \tag{21}$$

$$\phi_{II,j}^A=\lambda_{2j-1}^B=\prod_{k=1}^{j-2}[i\gamma_{2k-1}^A\gamma_{2k}^B](i\gamma_j^A\gamma_j^A), \tag{22}$$

$$\phi_{II,j}^B=\lambda_{2j}^A=\prod_{k=1}^{j-3}[i\gamma_{2l-1}^A\gamma_{2l}^B](i\gamma_{j-1}^A\gamma_j^A), \tag{23}$$

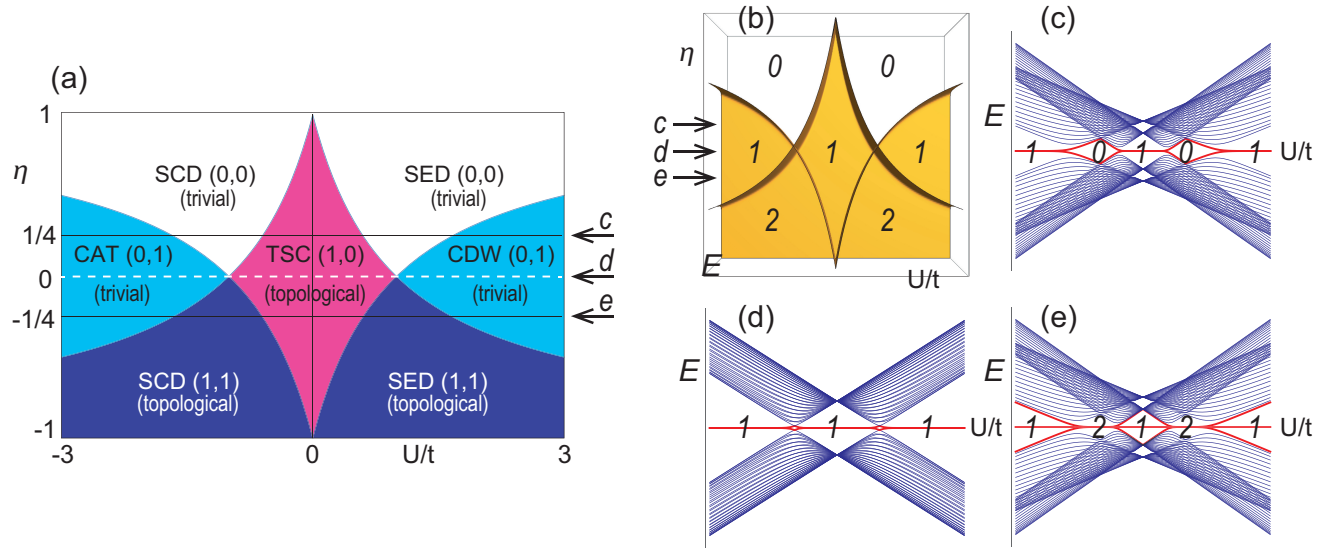

FIG. 2: (a) Topological phase diagram on the (U/t)-η plane. There are seven distinct phases indexed by (Q_I, Q_{II}), where Q_ν is the number of the type-ν edge states: Topological-superconductor (TSC), charge-density-wave (CDW), Schrödinger-cat (CAT), single-electron-dimer (SED) and superconducting-dimer (SCD) phases. (b) The low-energy edge spectrum on the (U/t)-η plane. Although there are edge states for the CDW and the CAT phases, they are bosonic and the systems are trivial. (c)–(e) The energy spectrum of a finite chain along the η line with $\eta = 1/4, 0, -1/4$, which is indicated by the arrow labelled by *c, d, e* in (a) and (b). Edge states are emphasized by red. The horizontal axis represents U/t, upon which the number of the zero-energy edge states is given for a semi-infinite chain. It is one half of that for a finite chain.

where we have defined $\gamma_j^A = c_j^\dagger + c_j$ and $\gamma_j^B = i(c_j^\dagger - c_j)$.

The zero-energy edge states of a semi-infinite chain are constructed[28,34] by operating the linear combination of the operators $Q_\nu^\mu = \sum_{j\geq 0} \alpha_{\nu,j} \phi_{\nu,j}^\mu$ to the Fock vacuum $|\text{vac}\rangle$, with $\mu = A, B$ and $\nu = I, II$, where the coefficients are given by[28]

$$\alpha_{I,j} = -\left(\frac{U(1+\eta)}{t(1-\eta)}\right)^j, \quad \alpha_{II,j} = -\left(\frac{t(1+\eta)}{U(1-\eta)}\right)^j. \tag{24}$$

The edge is either the A site or the B site, according to which we use the many-body Majorana operator Q_ν^A or Q_ν^B.

The condition for the convergence of the edge state is given by $|\alpha_{\nu,j}^\mu| < 1$ for $\nu = I$ and II. This is actually the condition for the emergence of the zero-energy edge state in Hamiltonian H_ν. For instance, if $|\alpha_{I,j}^\mu| > 1$ there is no zero-energy edge state in the Hamiltonian H_I. Hence, for each phase of the phase diagram we calculate (24) to decide whether $|\alpha_{\nu,j}^\mu| < 1$ or not, and determine the number Q_ν of the type-ν edge states. We show the results in the phase diagram as in Fig.2(a).

Topological properties: The Hamiltonian (1) does not conserve the fermion number $N = \sum_j c_j^\dagger c_j$ due to the superconducting pairing term but conserves the fermion parity[23–25,28,35] defined by $Z_2^f = (-1)^N$ since the superconducting paring term only changes the fermion number by two. It commutes (anticommutes) with any product of an even (odd) number of fermion operators. It is rewritten in terms of the Majorana operator as $Z_2^f = \prod_j i\gamma_j^A \gamma_j^B$. We find that $\{Q_I^\mu, Z_2^f\} = 0$ and $[Q_{II}^\mu, Z_2^f] = 0$. Hence, the type-I edge states are fermionic, while the type-II edge states are bosonic.

According to the bulk-edge correspondence, zero-energy edge states necessarily emerge if the system is topological but the reverse is not true. On one hand, it follows from (24) that the type-I edge state is adiabatically connected to a non-interacting Majorana zero-energy state as $U \to 0$, where it is shown to be topological based on the well-defined topological argument. On the other hand, since the type-II edge state disappears except for the $\eta = -1$ case, it is connected to a trivial state as $U \to 0$. It is bosonic, as we have mentioned. Consequently, the system with the type-I edge state is topological, while that with the type-II edge state is trivial[28].

TSC, CDW and CAT phases: We have found seven distinct phases. We investigate their topological and ground-state properties more in details. First, we focus on the three phases along the $\eta = 0$ line in Fig.2(a). They are already known[24] and named the topological-superconductor (TSC), charge-density-wave (CDW) and Schrödinger-cat (CAT) phases. The Schrödinger-cat state is a superposition of two superconducting states with different occupation numbers[24]. These ground-state properties are extended into the two-dimensional regions as in Fig.2(a) for $\eta \neq 0$, and hence we use the same names also for the two-dimensional phases. We note that the points $(U/t, \eta) = (\pm 1, 0)$ are tetra-critical points at which four distinct phases touch. It has been shown[13–16,24] that the TSC phase is topological while the CDW and CAT phases are trivial, which are consistent with the present results.

Dimer state: There are four phases which are absent for $\eta = 0$. We name them as the single-electron-dimer (SED) phases, and the superconducting-dimer (SCD) phases by the ground-state properties. Their ground-state properties and topological properties are made manifest in the strong dimerization limit $\eta = \pm 1$.

For $\eta = 1$ the system is separated into independent dimers as in Fig.1(a). The Hamiltonian (1) reads $H = \sum_j H_{2j-1,2j}$,

where for instance we have

$$H_{1,2} = -t\left[c_1^\dagger c_2 + c_2^\dagger c_1\right] - \Delta\left[c_1^\dagger c_2^\dagger + c_2 c_1\right] + U\left(2c_1^\dagger c_1 - 1\right)\left(2c_2^\dagger c_2 - 1\right). \quad (25)$$

The diagonalization is straightforward[23]. We note that, since the two-site Hamiltonian commutes with the fermion parity operator Z_2^f, the Hilbert space is decomposed into two subspaces containing even or odd numbers of electrons.

The even subspace is composed of the following two states,

$$|00\rangle \equiv |\text{vac}\rangle \text{ and } |11\rangle \equiv c_1^\dagger c_2^\dagger |\text{vac}\rangle, \quad (26)$$

corresponding to there are no electrons or two electrons. The Hamiltonian in the basis of $\{|00\rangle, |11\rangle\}$ is given by

$$H = \begin{pmatrix} U & -\Delta \\ -\Delta & U \end{pmatrix}, \quad (27)$$

which yields the energy dispersion $E_\pm^{\text{even}} = U \mp \Delta$ with the eigenfunction $\psi_\pm^{\text{even}} = \frac{1}{\sqrt{2}}(|00\rangle \pm |11\rangle)$.

The odd subspace is composed of the following two states,

$$|10\rangle \equiv c_1^\dagger |\text{vac}\rangle \text{ and } |01\rangle \equiv c_2^\dagger |\text{vac}\rangle, \quad (28)$$

corresponding to two one-electron states occupying the first site or the second site. The Hamiltonian in the basis of $\{|10\rangle, |01\rangle\}$ is given by

$$H = \begin{pmatrix} -U & -t \\ -t & -U \end{pmatrix}, \quad (29)$$

which yields the energy dispersion $E_\pm^{\text{odd}} = -U \mp t$ with the eigenfunction $\psi_\pm^{\text{odd}} = \frac{1}{\sqrt{2}}(\pm|10\rangle + |01\rangle)$.

We may derive the following results. On one hand, when the interaction is repulsive ($U > 0$), the ground state is a symmetric single electron hopping state $\psi_+^{\text{odd}} = \frac{1}{\sqrt{2}}(|10\rangle + |01\rangle)$ with the energy $E_+^{\text{odd}} = -U - t$. It is reasonable to call it the SED state. On the other hand, when the interaction is attractive ($U < 0$), it is a symmetric superconducting state $\psi_+^{\text{even}} = \frac{1}{\sqrt{2}}(|00\rangle + |11\rangle)$ with the energy $E_+^{\text{even}} = U - \Delta$. Since the state contains a pair of electrons, it is reasonable to call it the SCD state. Since there exist no zero-energy states, the system is topologically trivial.

For $\eta = -1$ the semi-infinite chain system is separated into independent dimers and an extra single site at the edge, as in Fig.1(e). The analysis of the dimer parts is precisely the same as in the limit $\eta = 1$. The single electron at the edge plays a key role, since its energy is zero in the absence of the chemical potential ($\mu = 0$). There exist two zero-energy states; the state $|0\rangle = |\text{vac}\rangle$ is bosonic, while the state $|1\rangle = c_1^\dagger |\text{vac}\rangle$ is fermionic. The emergence of the fermionic zero-energy state is a manifestation of the topological nontriviality of the system.

These basic properties remain almost as they are for $\eta \neq \pm 1$. At least in the region near $\eta = \pm 1$, the ground state is a linear superposition of individual dimers [Fig.1(b) and (d)]. There are trivial dimer phases for $\eta > 0$, while there are topological dimer phases for $\eta < 0$, which is differentiated by the emergence of the zero-energy edge state, as shown in Fig.2(c)–(e). We find there is no zero-energy state for $\eta > 0$, while there are two zero-energy states per one edge for $\eta < 0$, which are the type-I and the type-II edge states. In the topological phase, there is an unpaired site at the edge of a semi-infinite chain [Fig.1(d) and (e)], which results in the zero-energy edge states. We note that the topological and trivial phases alter once we take a half-shifted unit cell, which is a reminiscence of the SSH model[26].

Duality: The system has several duality relations[1,36]. The system (10) with $\eta = 0$ is self-dual[24] for $U = t$. We generalize it to the case that $\eta \neq 0$. The Hamiltonian (17) is invariant under the duality transformation, $t \leftrightarrow U$ and $\lambda_j^A \leftrightarrow \lambda_j^B$. For $\eta = 0$, there is only one transition point for $U/t > 0$, where the self-duality determines the transition point[24] as $U = t$. For $\eta \neq 0$, there are two transition points at $\eta = \pm(t - U)/(t + U)$ corresponding to (16), which are exchanged by the duality transformation.

The Hamiltonian is invariant also under the duality transformation, $t \leftrightarrow -U$ and $\lambda_j^A \leftrightarrow (-1)^j \lambda_j^B$, for which a similar argument follows. For $\eta = 0$, there is only one transition point for $U/t < 0$, where the self-duality determines the transition point as $U = -t$. For $\eta \neq 0$, there are two transition points at $\eta = \pm(t + U)/(t - U)$ corresponding to (16), which are exchanged by the duality transformation.

Finally, the Hamiltonian is invariant also under the duality transformation, $U \leftrightarrow -U$ and $\lambda_j^B \leftrightarrow (-1)^j \lambda_j^B$. For $\eta \neq \pm 1$, there are two transition points, $U/t = (1 \pm \eta)/(1 \mp \eta)$ and $-(1 \pm \eta)/(1 \mp \eta)$ corresponding to (16), which are exchanged by the duality transformation (the upper signs for $\mu > 0$ and the lower signs for $\mu < 0$). For $\eta = \pm 1$, there is only one transition point at $U/t = 0$, where the system is self-dual.

The author is very much grateful to N. Nagaosa, J.H.H. Perk, H. Katsura and J. Knolle for helpful discussions on the subject. This work is supported by the Grants-in-Aid for Scientific Research from MEXT KAKENHI (Grant Nos.JP17K05490 and JP15H05854). This work is also supported by CREST, JST (JPMJCR16F1).

Note added: After submission of the manuscript, a closely related paper[37] was uploaded in cond-mat/arXiv, where an exact solution on a similar interacting dimerized topological superconductor is obtained by using the same method. There is a difference between the two models that the interaction U is not dimerized in the above paper. Their results are consistent with ours.

[1] B. Kaufman, Phys. Rev. 76, 1232 (1949).
[2] P. Jordan and E. Wigner, Zeitschrift fur Physik 47, 631 (1928).
[3] R. Brauer and H. Weyl, American Journal of Mathematics 57, 425 (1935).
[4] J. Alicea, Rep. Prog. Phys. 75, 076501 (2012).
[5] C. W.J. Beenakker, Annu. Rev. Condens. Matter Phys. 4, 113 (2013).
[6] S.R. Elliott and M. Franz, Rev. Mod. Phys. 87, 137 (2015).
[7] C. Nayak, S. H. Simon, A. Stern, M. Freedman, and S. D. Sarma, Rev. Mod. Phys. 80, 1083 (2008).
[8] A. Yu. Kitaev, Phys. Usp. 44, 131 (2001).
[9] L. Fidkowski and A. Kitaev, Phys. Rev. B 81, 134509 (2010).
[10] S. Gangadharaiah, B. Braunecker, P. Simon, and D. Loss, Phys. Rev. Lett. 107, 036801 (2011).
[11] E.M. Stoudenmire, J.Alicea, O.A. Starykh, and M.P. A. Fisher, Phys. Rev. B 84, 014503 (2011).
[12] R. M. Lutchyn and M. P.A. Fisher, Phys. Rev. B 84, 214528 (2011).
[13] E. Sela, A. Altland, and A. Rosch, Phys. Rev. B 84, 085114 (2011).
[14] M. Cheng and H. H. Tu, Phys. Rev. B 84, 094503 (2011).
[15] F. Hassler and D. Schuricht, New J. Phys. 14, 125018 (2012).
[16] R. Thomale, S. Rachel, and P. Schmitteckert, Phys. Rev. B 88, 161103 (2013).
[17] A. Manolescu, D. C. Marinescu, and T.D. Stanescu, J. Phys. Condens. Matter 26, 172203 (2014).
[18] Y.H. Chan, C. K. Chiu, and K. Sun, Phys. Rev. B 92, 104514 (2015).
[19] J. Klassen and X. G. Wen, J. Phys. Condens. Matter 27, 405601 (2015).
[20] A. Rahmani, X. Zhu, M. Franz, and I. Affleck, Phys. Rev. Lett. 115, 166401 (2015).
[21] J.-J. Miao, H. -K. Jin, F.-C. Zhang, and Y. Zhou, cond-mat/arXiv:1608.08382.
[22] N. M. Gergs, L. Fritz, and D. Schuricht, Phys. Rev. B 93, 075129 (2016).
[23] H. Katsura, D. Schuricht, and M. Takahashi, Phys. Rev. B 92, 115137 (2015).
[24] J.-J. Miao, H.-K. Jin, F.-C. Zhang, and Y. Zhou, Phys. Rev. Letters 118, 267701 (2017).
[25] M. McGinley, J. Knolle, and A. Nunnenkamp, cond-mat/arXiv:1706.10249.
[26] W. P. Su, J. R. Schrieffer, and A. J. Heeger, Phys. Rev. Lett. **42**, 1698 (1979).
[27] R. Wakatsuki, M. Ezawa, Y. Tanaka and N. Nagaosa, Phys. Rev. B 90, 014505 (2014).
[28] P. Fendley, J. Stat. Mech. (2012) P11020.
[29] J.H.H. Perk, H.W. Capel, M.J. Zuilhof and Th.J. Siskens, Physica A 81, 319-348 (1975): J.H.H. Perk and H. Au-Yang, J. Stat. Phys. 135, 599-619 (2009).
[30] T. D. Schultz, D. C. Mattis, and E. H. Lieb, Rev. Mod. Phys. 36, 856 (1964).
[31] M. Greiter, V. Schnells, R. Thomale, Annals of Physics 351, 1026 (2014).
[32] R. Jullien and J. N. Fields, Phys. Lett. A 69, 214 (1978).
[33] H.W. Capel and J.H.H. Perk, Physica A 77, 211-242 (1977); J.H.H. Perk and H.W. Capel, Physica A 79, 265-303 (1977); J.H.H. Perk, H.W. Capel and Th.J. Siskens, Physica A 79, 304-325 (1977).
[34] G. Kells, Phys. Rev. B 92, 155434 (2015).
[35] A. M. Turner, F. Pollmann, and E. Berg Phys. Rev. B 83, 075102 (2011)
[36] L. Onsager, Phys. Rev. 65, 117 (1944).
[37] Y. Wang, J.-J. Miao, H.-K. Jin and S. Chen, cond-mat/arXiv:1707.08430.